scientific reports

Check for updates

OPEN

# Design of a novel long-acting insulin analogs by acetylation modification and compared with insulin Icodec

Min Yu[1,2], Chuanzhi Zhang[2], Hongjiang Xu[2], Yuanzhen Dong[1,3], Hongxiang Zhu[1], Chunguang Xia[2] & Jun Feng[1,3]✉

**Insulin is a potent medication for managing diabetes, yet its short half-life requires daily administration. Currently, Novo Nordisk's icodec is the sole insulin available on the market that requires administration only once a week. Insulin icodec, developed by Novo Nordisk through amino acid mutations and fatty acid side chain modifications, has demonstrated the capability to control blood glucose levels on a once-weekly basis. To improve its efficacy, we modified the acylation side chain of icodec to generate insulin analogs appropriate for weekly dosing. A promising insulin analog, TBE001-A-S033, was synthesized and conjugated, and its efficacy was assessed in ICR and db/db mice. TBE001-A-S033 prolonged blood glucose control in ICR mice and exhibited a comparable blood glucose trend to insulin icodec in db/db mice. These findings suggest that TBE001-A-S033 possesses a favorable hypoglycemic effect and a differential half-life across species compared to insulin icodec, indicating its potential for once-weekly use in humans. This preclinical investigation indicates that TBE001-A-S033 may serve as an effective therapeutic for type 2 diabetes mellitus (T2DM).**

**Keywords** Insulin analogs, Long-acting, Fatty acid

**Abbreviatons**

| | |
|---|---|
| AUC | Area under the curve |
| DELFIA | Dissociationenhanced-lanthanide fluoroimmunoassay |
| DMSO | Dimethyl sulfoxide |
| DMEM | Dulbecco's modified eagle medium |
| EDTA | Ethylene diamine tetraacetic acid |
| Fmoc | 9-Fluorenylmethyl chloroformate |
| HAC | Acid glacial |
| HAS | Human serum albumin |
| HbA1c | HemoglobinA1c |
| $IC_{50}$ | Half maximal inhibitory concentration |
| IR | Insulin receptor |
| LC-MS | Liquid chromatograph-mass spectrometer |
| LC-MS/MS | Liquid chromatography tandem mass spectrometry |
| MTX | Methotrexate |
| PBS | Phosphate buffer saline |
| PK | Pharmacokinetics |
| RP-HPLC | Reverse phase high-performance liquid chromatography |
| SPS | Solid-phase synthesis |
| STZ | Streptozotocin |
| TFA | Trifluoroacetic acid |
| $T_{1/2}$ | Half-life |
| T2DM | Type 2 diabetes mellitus |

[1]China State Institute of Pharmaceutical Industry, Shanghai, People's Republic of China. [2]Chia Tai Tianqing Pharmaceutical Group Co., Ltd, Lianyungang, Jiangsu, People's Republic of China. [3]Shanghai Duomirui Biotechnology Ltd, No.285 Gebaini Road, Pudong New Area, Shanghai 201203, China. ✉email: fengjdmr@163.com

Diabetes and its related complications are swiftly becoming a global health challenge. Patients with this condition typically require external assistance to attain glucose homeostasis[1,2]. Diabetes mellitus is a metabolic disorder characterized by hyperglycemia, which results from defects in insulin secretion or insulin action[3]. Persistent hyperglycemia and chronic metabolic disorders can lead to serious complications, including impairments and failures of the eyes, kidneys, cardiovascular system, and nervous system[4,5]. Insulin therapy remains a cornerstone of diabetes management, particularly for patients with type 1 diabetes and advanced type 2 diabetes. However, conventional insulin therapies are associated with challenges such as the risk of hypoglycemia, frequent injections, and suboptimal glycemic control due to the short duration of action and variability in absorption. To address these limitations, insulin analogs with modified amino acid sequences and structures have been developed, offering improved pharmacokinetic and pharmacodynamic profiles. Rapid-acting analogs (e.g., lispro and aspart) provide better postprandial glucose control, while long-acting analogs (e.g., detemir, glargine, and degludec) offer more stable basal insulin coverage with a reduced risk of hypoglycemia[1,6]. Despite these advancements, the need for daily injections remains a significant burden for patients, impacting adherence and overall treatment outcomes. Recently, insulin icodec, a once-weekly insulin analog, has emerged as a groundbreaking innovation, potentially transforming diabetes management by reducing injection frequency and improving patient convenience[7].

In recent years, researchers have employed four primary strategies to modify protein molecules and enhance their properties: chemical modification, protein engineering, fusion proteins, and protein glycosylation[8–11]. The popular insulin drugs, such as insulin glargine, insulin detemir, and insulin degludec, share common features that involve amino acid mutations and fatty acid modifications[12–16]. These drugs consist of four components: the insulin core, fatty acids, linkers, and spacers. The insulin backbone is responsible for the hypoglycemic effect and half-life, while the fatty acids facilitate binding to HSA. Linkers introduce negative charges to enhance hydrophilicity, and spacers provide necessary space to prevent interference with the spatial structure between insulin receptors and HSA. It is well established that HSA binding also influences the drug's half-life[17,18]. Therefore, various strategies have been employed to develop long-acting insulin formulations.

First, amino acid mutations can enhance protein stability, solubility, and insulin receptor (IR) affinity. Additionally, fatty acid modifications increase the affinity to HSA, thereby prolonging the half-life of the insulin analog[16]. The modification of fatty acids facilitates a slower and more sustained release, resulting in no significant plasma peak, a drug release profile more akin to basal insulin secretion, and a reduced risk of nocturnal hypoglycemia. However, these drugs have not yet attained a one-weekly dosing regimen[14,15,19–21].

Recently, Novo Nordisk developed insulin icodec, a new insulin analog designed for once-weekly dosing, which has garnered widespread attention[1,22,23]. Insulin icodec features three amino acid substitutions (A14E, B16H, and B25H) that enhance molecular stability and contribute to reduced insulin IR binding and clearance, thereby prolonging its half-life. Additionally, the incorporation of a C20 fatty diacid-containing side chain confers strong, reversible binding to HSA[1,6,24]. It has been reported that the combination of A14E and B25H substitutions can significantly enhance the solubility of insulin analogs, allowing for preparations with concentrations up to 7 times higher than standard U700 insulin[24]. The threonine at position B30 of human insulin was removed as it does not affect IR affinity. In summary, the mutations of three amino acids increased molecular stability, decreased IR binding, and enhanced solubility. These modifications not only prolong the half-life but also enable a once-weekly dosing regimen, addressing a critical unmet need in diabetes care.

Additionally, the incorporation of a fatty acid side chain facilitates strong yet reversible binding to HSA, while amino acid substitutions enhance molecular stability and contribute to prolonged half-life. Various fatty acid side chains were explored, each yielding distinct half-life profiles[1]. This suggests that appropriate modifications to the fatty acid side chain, in conjunction with amino acid substitutions, may result in improved insulin analogs.

Despite the success of insulin icodec, there is ongoing interest in further optimizing insulin analogs to achieve even longer durations of action, improved glycemic control, and reduced side effects. This study aimed to develop a novel long-acting insulin analog by acetylating the insulin icodec main chain and exploring various fatty acid side chains. Using solid-phase synthesis (SPS), we synthesized and attached different fatty acid side chains to the insulin icodec main chain. The biological activity of these analogs was evaluated through in vitro bioactivity assays and in vivo studies in ICR and db/db mice. Among the synthesized analogs, TBE001-A-S033, featuring a C22 diacid-2γGlu-2OEG conjugation at the B29k position, demonstrated superior HSA affinity and effective blood sugar reduction in murine models. However, its half-life in Beagle dogs was slightly shorter than that of insulin icodec. These findings highlight the potential of targeted modifications to develop next-generation insulin analogs with improved therapeutic profiles, ultimately enhancing patient outcomes and quality of life.

## Results

### Obtained insulin analogs main chain

Based on the advantages of insulin icodec over other insulin analogs, we selected the insulin icodec main chain as our starting point, as illustrated in Fig. 1. A recombinant Pichia pastoris strain, designated P. pastoris *TBE001-A*, expressing the precursor of the insulin icodec main chain was constructed and preserved in our laboratory. The precursor of the insulin icodec main chain was obtained through the fermentation of P. pastoris *TBE001-A*. Following purification, the insulin icodec main chain was obtained with a purity exceeding 95%, as confirmed by LC-MS (Figure SI-1, Supporting Information). The purified insulin icodec main chain was then used for further modification with fatty acid side chains.

### Design fatty acid sides chains and synthesis of the insulin analogs

The modifications to the fatty acid side chains of insulin icodec impart strong yet reversible HSA affinity, while amino acid substitutions enhance molecular stability and contribute to clearance. These variations in fatty acid


**Fig. 1**. Insulin icodec main chain.

| Insulin analogs | Fatty acid sides | | | Purity | Molecular mass | |
|---|---|---|---|---|---|---|
| | Fatty diacid | Linker | Intervals | | Calculated | Observed |
| Insulin icodec | C20 | γGlu | 2*OEG | 91.74 | 6380.3 | 1276.7000[M + 5 H]$^{5+}$ |
| TBE001-A-S004 | C20 | 2*γGlu | OEG | 91.57 | 6364.3 | 1273.8000[M + 5 H]$^{5+}$ |
| TBE001-A-S005 | C20 | 3*γGlu | OEG | 89.33 | 6493.4 | 1299.6000[M + 5 H]$^{5+}$ |
| TBE001-A-S006 | C20 | 4*γGlu | OEG | 97.67 | 6622.6 | 1325.5000[M + 5 H]$^{5+}$ |
| TBE001-A-S007 | C20 | 2*γGlu | 2*OEG | 85.65 | 6509.5 | 1302.8000[M + 5 H]$^{5+}$ |
| TBE001-A-S008 | C20 | 2*γGlu | 3*OEG | 94.88 | 6654.6 | 1331.9000[M + 5 H]$^{5+}$ |
| TBE001-A-S009 | C20 | 3*γGlu | 2*OEG | 94.11 | 6638.6 | 1328.7000[M + 5 H]$^{5+}$ |
| TBE001-A-S010 | C20 | 4*γGlu | 2*OEG | 93.03 | 6767.8 | 1354.5000[M + 5 H]$^{5+}$ |
| TBE001-A-S014 | C20 | γGlu | 3*OEG | 92.46 | 6525.5 | 1305.7000[M + 5 H]$^{5+}$ |
| TBE001-A-S015 | C20 | γGlu | 4*OEG | 92.41 | 6670.7 | 1334.8000[M + 5 H]$^{5+}$ |
| TBE001-A-S029 | C22 | 2*γGlu | OEG | 91.46 | 6392.3 | 1279.2000[M + 5 H]$^{5+}$ |
| TBE001-A-S030 | C22 | 3*γGlu | OEG | 96.97 | 6521.5 | 1304.9000[M + 5 H]$^{5+}$ |
| TBE001-A-S031 | C22 | γGlu | 2*OEG | 93.87 | 6408.4 | 1282.7000[M + 5 H]$^{5+}$ |
| TBE001-A-S033 | C22 | 2*γGlu | 2*OEG | 92.84 | 6537.5 | 1308.1000[M + 5 H]$^{5+}$ |
| TBE001-A-S040 | C18 | 2*γGlu | OEG | 98.42 | 6336.2 | 1268.3000[M + 5 H]$^{5+}$ |
| TBE001-A-S041 | C18 | 3*γGlu | OEG | 97.00 | 6465.4 | 1294.0000[M + 5 H]$^{5+}$ |
| TBE001-A-S042 | C18 | γGlu | 2*OEG | 98.05 | 6352.3 | 1271.5000[M + 5 H]$^{5+}$ |
| TBE001-A-S043 | C18 | 2*γGlu | 2*OEG | 93.73 | 6481.4 | 1297.2000[M + 5 H]$^{5+}$ |

**Table 1**. Fatty side chains and insulin analogs.

side chains result in different half-lives. Based on the insulin icodec structure, we designed a variety of fatty acid side chains, which include three components: fatty diacid, linker, and spacer, as depicted in Table 1 (Figure SI-2-20, Supporting Information). The structures of the fatty diacids, linker, spacer, and the synthesis scheme for TBE001-A-S033 are illustrated in Fig. 2A and B, respectively.

## In vitro bioactivity and HSA affinity assays

To assess the impact of the designed fatty acid side chains on the in vitro bioactivity of insulin analogs, particularly their HSA affinity, which can facilitate the development of long-acting formulations, we conducted a series of experiments. The results, summarized in Table 2, indicate that the insulin analogs exhibit minor differences in vitro bioactivity. However, significant variations were observed in their affinity for HSA. These findings suggest that while the bioactivity remains relatively consistent, the structural modifications introduced by the fatty acid side chains significantly influence HSA binding.

These results indicate that variations in the fatty diacid type, linkers, and spacers within the fatty acid side chains lead to distinct effects on in vitro bioactivity and HSA affinity. Specifically, the data show that in vitro bioactivity is predominantly determined by the insulin main chain, while HSA affinity is primarily influenced by modifications to the fatty acid side chains of the insulin main chain. These findings highlight the differential roles of structural components in modulating bioactivity and HSA binding.

Table 2 illustrates that as the carbon chain length of the fatty diacid in the fatty acid side chain increases, a higher HSA affinity is observed. Specifically, insulin analogs with a C22 diacid fatty chain show the highest HSA affinity among the tested compounds. These data provide a basis for further investigation into the relationship between fatty acid side chain structure and HSA binding properties.

Compared with insulin icodec, TBE001-A-S014, and TBE001-A-S015 exhibit increased OEG content and higher HSA affinity. This trend is consistent across insulin analogs with C18 (TBE001-A-S040, TBE001-A-S043), C22 (TBE001-A-S029, TBE001-A-S030), and C22 (TBE001-A-S004, TBE001-A-S007, TBE001-A-S008, TBE001-A-S005, TBE001-A-S009, TBE001-A-S006, TBE001-A-S010) fatty diacid carbon chains.

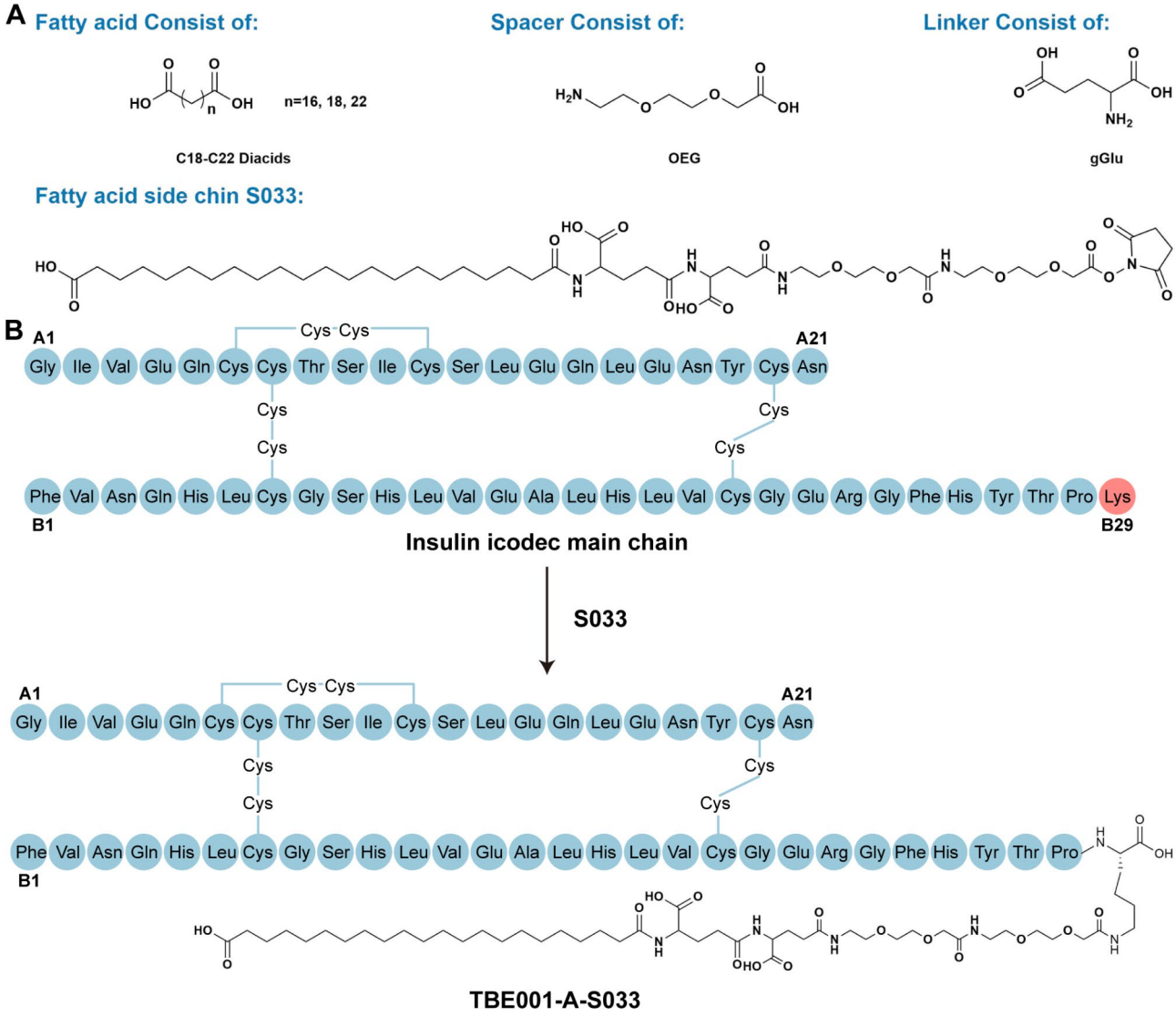


**Fig. 2**. (**A**) Structures of fatty acids, linker, spacer and fatty acid side chain. (**B**) Scheme for the synthesis of TBE001-A-S033.

Compared with insulin icodec, TBE001-A-S07, TBE001-A-S09, and TBE001-A-S010 exhibit reduced γGlu content and increased HSA affinity. This trend is consistent across insulin analogs with C18 (TBE001-A-S040, TBE001-A-S041, TBE001-A-S042, TBE001-A-S043), C22 (TBE001-A-S029, TBE001-A-S030, TBE001-A-S031, TBE001-A-S033), and C20 (TBE001-A-S004, TBE001-A-S005, TBE001-A-S006, TBE001-A-S008, TBE001-A-S014) fatty diacid carbon chains.

Based on these findings, insulin analogs TBE001-A-S006, TBE001-A-S008, TBE001-A-S010, TBE001-A-S014, TBE001-A-S015, TBE001-A-S029, TBE001-A-S030, TBE001-A-S031, and TBE001-A-S033, which demonstrated enhanced HSA affinity, were selected for further experimentation.

## In vivo study in ICR mice

To further evaluate the insulin analogs TBE001-A-S006, TBE001-A-S008, TBE001-A-S010, TBE001-A-S014, TBE001-A-S015, TBE001-A-S029, TBE001-A-S030, TBE001-A-S031, and TBE001-A-S033, pharmacodynamic studies were conducted. These analogs were selected based on their HSA affinity, which exceeded 90% compared to insulin icodec. The studies were performed using ICR mice at a dose of 1.44 μmol/kg via subcutaneous injection. ICR mice demonstrate a pronounced sensitivity to dietary and environmental changes in their metabolic responses, making them highly suitable for modeling physiological and pathological alterations in human glucose regulation. This attribute positions them as an exemplary model for studying blood glucose levels, insulin sensitivity, and diabetes-related mechanisms. The results are presented in Fig. 3.

As depicted in Fig. 3A, five insulin analogs—TBE001-A-S015, TBE001-A-S029, TBE001-A-S030, TBE001-A-S031, and TBE001-A-S033—exhibited prolonged blood glucose control compared to insulin icodec. Among these analogs, TBE001-A-S029 and TBE001-A-S033 showed significantly different AUC0-72 h values relative to

| Insulin analogs | $EC_{50}a/EC_{50}b$ Relative to insulin icodec | HSA affinity Relative to insulin icodec |
|---|---|---|
| Insulin icodec | 1 | 100.0 |
| TBE001-A-S004 | 6.1 | 87.9 |
| TBE001-A-S005 | 1.9 | 83.8 |
| TBE001-A-S006 | 3.4 | 79.9 |
| TBE001-A-S007 | 0.6 | 83.8 |
| TBE001-A-S008 | 1.1 | 98.9 |
| TBE001-A-S009 | 3 | 88.2 |
| TBE001-A-S010 | 3.3 | 91.2 |
| TBE001-A-S014 | 1.1 | 109.5 |
| TBE001-A-S015 | 1.2 | 110.5 |
| TBE001-A-S029 | 8.6 | 121.1 |
| TBE001-A-S030 | 6.6 | 120.7 |
| TBE001-A-S031 | 2.1 | 136.0 |
| TBE001-A-S033 | 1.3 | 123.0 |
| TBE001-A-S040 | 2.4 | 54.7 |
| TBE001-A-S041 | 3.1 | 39.0 |
| TBE001-A-S042 | 1.4 | 76.6 |
| TBE001-A-S043 | 0.9 | 66.6 |

**Table 2**. In vitro bioactivity and HSA affinity of the insulin analogs.

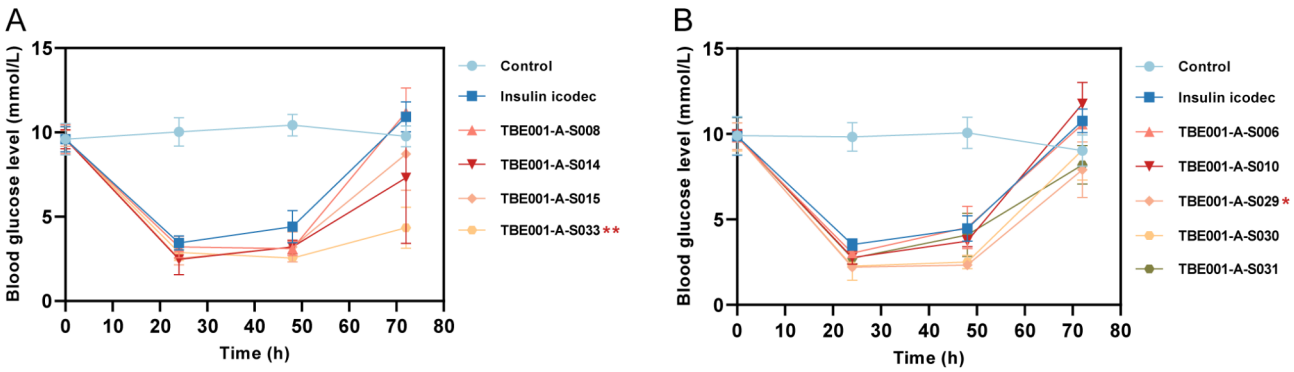


**Fig. 3**. Biological activity in normal (ICR) mice. Calculated plasma glucose AUC0-72 h; Data are given as the mean ± SD, $n = 4$. Differences were determined using one-way ANOVA followed by Dunnett's test to compare treatment effects versus the vehicle control group. $p < 0.1$,*$p < 0.05$, **$p < 0.01$, ***$p < 0.001$, ****$p < 0.0001$ versus insulin icodec.

insulin icodec, with TT test results of 0.024 and 0.003, respectively. Due to its superior performance in both in vitro and in vivo studies, TBE001-A-S033 was selected for further evaluation of its in vivo biological activities in db/db mice.

## In vivo study in Db/db mice

To further evaluate the pharmacodynamic profile of TBE001-A-S033, an insulin analog selected based on its AUC0-72 h performance, a study was conducted using db/db mice. Db/db mice are extensively utilized in diabetes and related metabolic disease research, with their pathological features and experimental responses thoroughly validated. These mice received subcutaneous injections of either 3 mg/kg or 6 mg/kg of TBE001-A-S033 every two days. The results are presented in Fig. 4. TBE001-A-S033 exhibited a similar blood glucose trend to insulin icodec but at a lower control level in db/db mice. The AUC11-48 h for TBE001-A-S033 was lower than that of insulin icodec (Fig. 4A). Additionally, TBE001-A-S033 demonstrated a clear advantage over insulin icodec in reducing HbA1c levels at both dosages (Fig. 4B).

## In vitro pharmacokinetics in different species

To further assess plasma stability and provide a foundation for subsequent in vivo pharmacokinetic studies, we evaluated the plasma stability of TBE001-A-S033 and insulin icodec across various species. The results, presented in Table 3, indicate that insulin icodec was unstable in mouse plasma after 48 h of incubation at 37 °C, whereas it remained stable in the plasma of rats, dogs, monkeys, and humans within the same timeframe. Similarly,

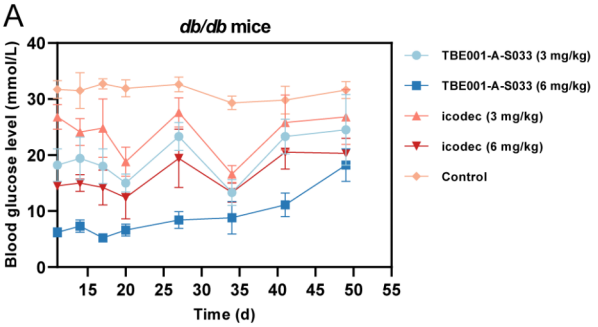


B

| Group | Dose (mg/kg) | HbA1c (%) | HbA1c (%) |
|---|---|---|---|
| Control | —— | 9.62 ± 0.73 | —— |
| TBE001-A-S033 | 3 | 8.85 ± 0.96 | -17.37 |
| TBE001-A-S033 | 6 | 7.95 ± 0.48 | -21.01 |
| icodec | 3 | 8.51 ± 0.39 | -7.96 |
| icodec | 6 | 7.62 ± 1.21 | -11.49 |

**Fig. 4**. Effects of TBE001-A-S033 and insulin icodec in db/db mice. (**A**) Blood glucose level, (**B**) HbA1c level. Data are given as the mean ± SD, $n = 4$.

| Species/compunds | Time (h) | Remaining compunds (%) | | | | |
|---|---|---|---|---|---|---|
| | | Mice | Rat | Dog | Monkey | Human |
| icodec | 0 | 100.00 | 100.00 | 100.00 | 100.00 | 100.00 |
| | 1 | 104.13 | 97.02 | 87.39 | 88.41 | 97.86 |
| | 4 | 94.08 | 96.48 | 95.97 | 98.92 | 97.10 |
| | 24 | 95.64 | 99.69 | 97.77 | 103.03 | 113.78 |
| | 48 | 82.89 | 96.39 | 88.82 | 89.76 | 101.25 |
| TBE001-A-S033 | 0 | 100.00 | 100.00 | 100.00 | 100.00 | 100.00 |
| | 1 | 96.87 | 93.64 | 87.90 | 93.45 | 93.06 |
| | 4 | 92.11 | 102.90 | 102.52 | 101.70 | 104.03 |
| | 24 | 77.74 | 109.94 | 100.96 | 111.75 | 99.42 |
| | 48 | 63.19 | 97.24 | 85.14 | 94.25 | 86.19 |

**Table 3**. Stability of Icodec and TBE001-A-S033 in plasma from different species.

TBE001-A-S033 demonstrated instability in mouse plasma after 24 h at 37 °C, but was stable in the plasma of rats, dogs, monkeys, and humans within 48 h.

## In vivo pharmacokinetics in beagle dogs and rats

Beagle dogs and SD rats were selected for in vivo pharmacokinetic studies. SD rats, with their moderate body size, are well-suited for procedures such as blood collection and drug administration, facilitating frequent sampling to monitor temporal changes in blood drug concentration. Beagle dogs, on the other hand, exhibit metabolic pathways and organ functions (e.g., liver and kidney) closely resembling those of humans, thereby offering a more accurate prediction of drug metabolism in humans. By utilizing SD rats and beagle dogs as small and large animal models, respectively, comprehensive pharmacokinetic data can be obtained from diverse perspectives. Comparative analysis of these two models enhances the consistency and reliability of experimental findings, thereby strengthening the scientific foundation for subsequent clinical trials.

To compare the pharmacokinetic profiles of icodec and TBE001-A-S033, rats were administered a subcutaneous injection of 2 mol/kg following a basal gavage. Figure 5A depicts the plasma drug concentration-time curves, and Table 4 presents the pharmacokinetic parameters. The data indicate that icodec achieved a maximum concentration of 69.9 ng/mL at 6.5 h post-injection, whereas TBE001-A-S033 reached a Cmax of 73.7 ng/mL at 8 h. Both drugs exhibited similar blood exposure levels. The half-life of TBE001-A-S033 was 17 h, compared to 18.9 h for icodec.

We then compared the pharmacokinetic profiles of the two compounds in beagle dogs. Figure 5B illustrates the plasma drug concentration-time curves, while Table 5 provides the relevant pharmacokinetic parameters. Following a single subcutaneous administration, TBE001-A-S033 was absorbed into the plasma, with a Tmax ranging from 8 to 24 h, an elimination half-life of 48.3 to 54.6 h, and a maximum plasma concentration of 93.9 ng/mL. In comparison, insulin icodec reached a maximum plasma concentration of 79.1 ng/mL within 6 to 24 h. The exposure level of TBE001-A-S033 was 1.036 times higher than that of insulin icodec, and the elimination rate of TBE001-A-S033 was 0.814 times faster than that of insulin icodec.

The incorporation of a fatty acid side chain to enhance HSA affinity is a proven strategy for prolonging the in vivo half-life of drugs. The pharmacokinetic characteristics of insulin analogs are intricately linked to the composition of the fatty diacid, linker, and spacer attached to the insulin backbone. In the case of insulin icodec, a C20 diacid is conjugated to the Lys residue at position 20 of the insulin molecule through a 2OEG spacer and a γGlu linker. The distinction between TBE001-A-S033 and insulin icodec lies in the former's possession of a longer fatty acid, a C22 diacid, and an extended linker, 2γGlu. The pharmacokinetic profile of TBE001-

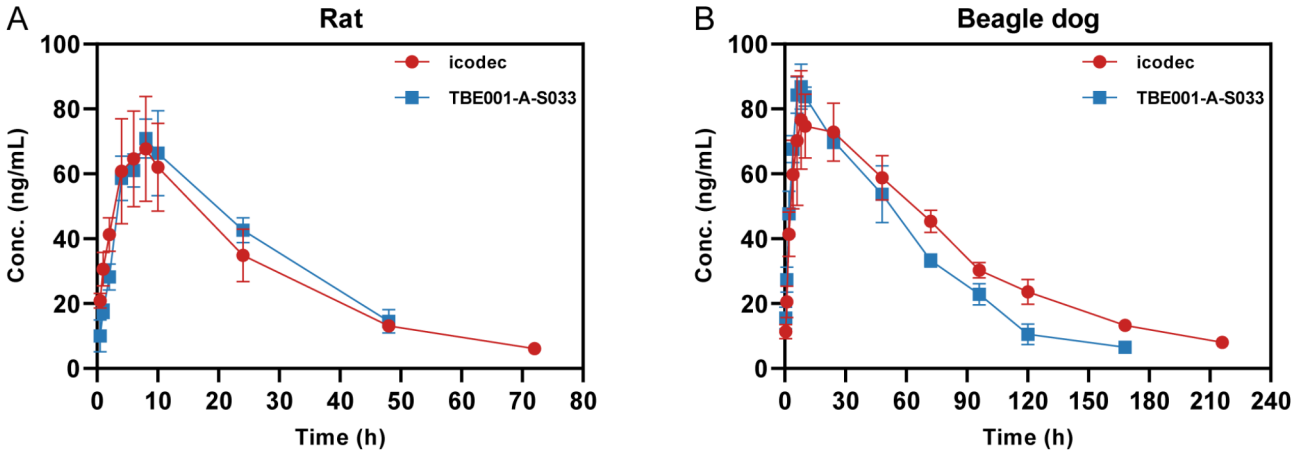


**Fig. 5**. Average plasma concentrations of TBE001-A-S033 and Insulin icodec in rat (**A**) and beagle dogs (**B**), after single subcutaneous injection at 2 nmol/kg.

| Analyst | Insulin icodec | TBE001-A-S033 |
|---|---|---|
| Tmax (h) | 6.50 ± 1.91 | 8.00 ± 1.63 |
| Cmax (ng/mL) | 69.9 ± 14.9 | 73.7 ± 9.43 |
| AUC0-168 h (h × ng/mL) | 2029 ± 391 | 1957 ± 240 |
| $t_{1/2}$ (h) | 18.9 ± 1.56 | 17.0 ± 1.28 |

**Table 4**. Pharmacokinetic parameters in rat.

| Analyst | Insulin icodec | TBE001-A-S033 |
|---|---|---|
| Tmax (h) | 11.5 ± 8.39 | 12.0 ± 8.16 |
| Cmax (ng/mL) | 79.1 ± 12.2 | 93.9 ± 18.7 |
| AUC0-168 h (h × ng/mL) | 6872 ± 574 | 7123 ± 530 |
| $t_{1/2}$ (h) | 61.9 ± 6.28 | 50.4 ± 2.9 |

**Table 5**. Pharmacokinetic parameters in beagle dogs.

A-S033 indicates differences in maximum plasma concentration, exposure level, and elimination rate compared to insulin icodec.

## Discussion

This study focuses on the development of a novel long-acting insulin analog derived from the icodec insulin structure, aiming to optimize glycemic control in patients with diabetes. The molecular design of icodec insulin integrates two critical modifications: (1) the incorporation of three specific amino acid substitutions (A14E, B16H, and B25H) within the insulin backbone, which enhances molecular stability, reduces insulin receptor (IR) binding affinity and clearance rate, and prevents the dissociation of the A and B chains, thereby extending the drug's half-life; and (2) the attachment of a fatty acid side chain at the C20 position, enabling reversible high-affinity binding to HSA and facilitating once-weekly administration[25]. Unlike traditional insulin backbone modifications, the fatty acid side chain approach provides a more efficient and practical method for achieving prolonged action[26]. Based on this framework, we designed and synthesized a series of analogs with diverse fatty acid side chain structures. Through in vitro bioactivity assays, HSA binding affinity evaluations, and comprehensive pharmacodynamic and pharmacokinetic studies, we identified candidate insulin analogs with optimal performance characteristics.

Our findings align with previous studies demonstrating that fatty acid side chain modifications significantly enhance the PK PD properties of insulin analogs[27,28]. However, our results extend these observations by systematically exploring the impact of side chain architecture on albumin binding affinity and bioactivity. Specifically, we found that elongating fatty acid side chains and increasing OEG content significantly enhance albumin binding, consistent with prior reports[29,30]. Notably, our study also revealed that γGlu content inversely correlates with HSA binding affinity, a finding that contrasts with some earlier studies[31]. This discrepancy may arise from differences in experimental conditions or the specific structural configurations of the analogs tested. These observations highlight the complexity of optimizing insulin analogs for both PK and PD properties. While

albumin binding is crucial for prolonging half-life, it may also introduce steric or conformational constraints that impair receptor binding. This trade-off underscores the need for a balanced approach in designing insulin analogs, as overly aggressive modifications to enhance albumin affinity may inadvertently compromise bioactivity.

To accomplish our research objectives while adhering to animal welfare principles, we optimized the experimental design by implementing a strategy to minimize animal usage for compound screening. Through systematic evaluations of HSA binding affinity and in vitro activity, nine insulin analogs were selected for comprehensive in vivo pharmacodynamic analysis. Initial screening results revealed that TBE001-A-S029 and TBE001-A-C033 exhibited significantly lower blood glucose AUC0-72 h values compared to other analogs, suggesting their superior glycemic control potential. Structural characterization revealed that both compounds feature a C22 fatty acid binding site and a double γGlu motif, differing solely in the number of OEG groups—a structural distinction potentially linked to their enhanced glycemic control efficacy[32]. This finding aligns with previous studies demonstrating that fatty acid modifications and γGlu motifs can significantly influence insulin's pharmacokinetic properties[33]. Further pharmacodynamic assessments highlighted the superior performance of TBE001-A-S033 in the TT test, likely due to its markedly higher in vitro biological activity relative to TBE001-A-S029[7]. Notably, TBE001-A-S033 demonstrated improved glycemic regulation in both ICR and db/db mouse models compared to icodec, consistent with its enhanced in vitro activity and structural stability.Cross-species plasma stability analyses further confirmed the consistent stability profiles of these compounds across species, suggesting their potential for translational applications.

Pharmacokinetic investigations revealed that TBE001-A-S033 exhibits a higher absorption rate than insulin icodec in both beagle dogs and rat models, with a 1.036-fold increase in exposure and a 0.814-fold reduction in elimination rate. These findings are consistent with previous reports on the role of structural modifications in modulating insulin absorption kinetics[6]. Of particular significance are the delayed Tmax and elevated Cmax observed with TBE001-A-S033, which likely contribute to its enhanced glycemic control. However, despite its greater albumin affinity, TBE001-A-S033 displayed a shorter half-life in rats and beagle dogs than icodec, a phenomenon that warrants further investigation. This observation contrasts with the conventional understanding that increased albumin binding typically prolongs half-life, suggesting the involvement of alternative clearance mechanisms, such as receptor-mediated uptake or tissue distribution[34].TBE001-A-S033 and icodec exhibit significantly longer half-lives compared to double-PEGylated insulin analogs, highlighting the superior efficacy of fatty acid modifications in extending drug duration[35]. In contrast, while TBE001-A-S033 and icodec demonstrate higher in vitro bioactivity than Fc-fused insulin analogs, their half-lives are comparatively shorter[36]. Our results are consistent with recent studies highlighting the importance of side chain modifications in optimizing insulin analogs[18]. However, the shorter half-life of TBE001-A-S033 compared to icodec, despite its higher albumin affinity, challenges the conventional assumption that increased albumin binding invariably extends half-life. This finding aligns with emerging evidence suggesting that receptor-mediated clearance mechanisms may play a more significant role in determining insulin analog half-life than previously thought.

The therapeutic potential of TBE001-A-S033 is significant, particularly in the context of improving glycemic control and enhancing patient adherence through a once-weekly subcutaneous injection regimen. However, we acknowledge the potential limitations of ultra-long-acting insulin preparations, including the risk of exacerbating insulin resistance in diabetic patients. This concern is particularly relevant given the growing body of literature highlighting the complex interplay between insulin therapy and insulin resistance[37]. The recent marketing authorization of icodec insulin by the European Commission provides a valuable opportunity to further assess the risk-to-benefit ratio of ultra-long-acting insulin analogs in a real-world setting[38]. As the number of users increases, more precise evaluations of clinical outcomes and potential side effects will be possible.

Despite these promising findings, our study has several limitations. First, the side chain design in this study utilizes conventional linker and spacer configurations, without exploring or extending alternative structural frameworks. Although this approach preserves the fundamental functional properties of the molecules, it restricts structural diversity, which may limit potential applications. Second, the preclinical models used may not fully recapitulate the metabolic and pharmacokinetic profiles of humans. Third, the relatively short duration of our in vivo studies limits our ability to assess long-term safety and efficacy. Finally, the absence of clinical data necessitates caution in extrapolating our findings to human patients. Future studies should address these limitations by incorporating longer-term preclinical assessments and initiating clinical trials to evaluate the safety, efficacy, and patient acceptability of TBE001-A-S033.

In conclusion, our study contributes to the growing body of knowledge on long-acting insulin analogs and highlights the importance of optimizing fatty acid side chains to achieve desired pharmaceutical attributes. Future research should focus on further elucidating the mechanisms underlying the PK and PD properties of acylated insulin analogs, as well as conducting comprehensive clinical trials to evaluate their long-term efficacy and safety. Additionally, incorporating oral glucose tolerance tests and glucose clamp techniques will provide a more precise assessment of TBE001-A-S033 and its potential as a therapeutic agent for diabetes.

## Materials and methods

### Materials

The 2-Chlorotrityl Chloride Resin (2-CTC Resin) was obtained from Sunresin New Materials Co., Ltd. (China). Fatty diacids were purchased from the Bidder Medical Platform (China). A variety of Fmoc-protected amino acids, Ninhydrin hydrate, 2,2,2-Trifluoroethanol (TFE), and N, N-Diisopropylethylamine (DIEA) were sourced from Energy Chemical (China). 1-Hydroxybenzotriazole (HOBt) was acquired from Phamablock Co., Ltd. (China). Dichloromethane (DCM), N-Methyl-2-pyrrolidone (NMP), N,N-Dimethylformamide (DMF), and Ethanol were all supplied by Nanjing Reagent Co., Ltd. (China). Piperidine (PIP) and Phenol were provided by Sinoreagent Co., Ltd., and N, N'-Diisopropylcarbodiimide (DIC) was purchased from Aladdin (China).

Methanol and acetonitrile sourced from Yunnan Xinlanjing Chemical Industry Co, Ltd (China). Sodium Pyruvate, MEM Non-Essential Amino Acids Solution, TrypLE™ Express, Dulbecco's Modified Eagle Medium (DMEM), and Fetal Bovine Serum (FBS) were all obtained from Gibco (USA); HSA was purchased from Beijing Solarbio Science & Technology Co., Ltd. (China). The Cell Extraction Buffer was bought from Invitrogen, another American supplier. Methotrexate and Bovine Serum Albumin (BSA) were sourced from Sigma (USA); Recombinant Human INSR protein was acquired from Sino biological (China). For filtration needs, the Hollow Fiber Filter Module was purchased from Spectrumlabs (USA). Chromatography equipment, including Waters Symmetry Shield RP8 (150 × 4.6 mm, 3.5 μm) and Waters ACQUITY UPLC BEH C8, were both procured from Waters (USA). SP Bestrose FF and NHS-activated Bestarose 4FF were obtained from Bestchrom (China). The centrifuge was purchased from Beckman Coulter, Inc (USA).The HPLCONE-10C8C2 was sourced from Daiso (Japan). N-Hydroxysuccinimide was provided by Binhai Hanhong Biochemical Co., LTD (China). CHO-hIR cells were purchased from GenScript Biotech (China). Lastly, the P. pastoris TBE001-A strain is preserved in our lab. Blank human, monkey, rat, mouse, and dog plasma samples were procured from Chia Tai Tianqing Pharmaceutical Group Co., Ltd. (China).

## In vitro studies

*Insulin analogs main chain*

The *P. pastoris* TBE001-A strain, maintained in our laboratory, was cultured in a 30-liter bioreactor. Target protein expression was induced by methanol, and the supernatant was harvested via centrifugation. The supernatant was subsequently filtered using a 750 kDa molecular-weight cutoff hollow fiber filter (Spectrumlabs, USA) to isolate the target protein. The filtrate was then concentrated using a 3 kDa molecular-weight cutoff membrane unit (Millipore, USA), and the buffer was exchanged for 20 mM sodium acetate at pH 4.0. Insulin precursors were purified through SPFF cation exchange chromatography. The resulting solution containing the insulin precursors underwent buffer exchange using a 1 kDa molecular-weight cutoff hollow fiber (Spectrumlabs, USA) to prepare for enzymatic digestion. Mature insulin was generated by enzymatic digestion with lysozyme at 37 °C overnight, followed by further purification using reverse-phase chromatography. The purified samples were subjected to an additional buffer exchange using a 1 kDa molecular-weight cutoff hollow fiber. The icodec main chain of insulin was isolated, achieving a purity level exceeding 97%, as confirmed by HPLC analysis (Agilent 1260-Bio, USA) on a Waters Symmetry Shield RP8 column (4.6 × 150 mm, 3.5 μm) with gradient elution (Phase A: 100 mM sodium sulfate, 100 mM PBS with 9.6% acetonitrile, pH 5.8; Phase B: acetonitrile-water [50:50]).

## Synthesis and activate of side chain

The fatty acid side chains were synthesized using SPS on 2-CTC resin with fatty diacids and Fmoc-protected amino acids. After synthesis, the fatty acid side chains were cleaved from the resin using a mixture of TFA and DCM (1:4, v/v) under agitation at 120 rpm for 1 h. The resulting fatty acid side chains were analyzed by HPLC (Shimadzu, LC-30 A, Japan) on a Waters ACQUITY UPLC BEH C8 column (2.1 mm × 100 mm, 1.7 μm) with gradient elution (Phase A: 0.1% formic acid in water; Phase B: 0.1% formic acid in acetonitrile).

Activate of the side chain: Excess HOSU and DCC were added to the synthetic side chain, and DCM was used as the solvent for mixing activation at room temperature for 1–2 h. The reaction mixture was stirred at room temperature for 1–2 h. After activation, the mixture was filtered through a 0.2 μm organic filter membrane, and the solvent was removed as thoroughly as possible using a vacuum centrifugal concentrator at 30 °C. The residue was suspended in ethyl acetate and filtered again through a 0.2 μm organic filter membrane. The solvent was removed using a vacuum centrifugal concentrator at 30 °C, and this process was repeated once. For deprotection, TFA was added in a volume exceeding 80% of the total mixture, and the reaction was allowed to proceed for 0.5–2 h to remove the protective groups. Isopropyl ether (8 times the volume of the mixture) was then added to induce precipitation at -20 °C for 10–30 min. After centrifugation at 8000 rpm for 5 min, the supernatant was discarded. The precipitate was washed with additional isopropyl ether, resuspended, and centrifuged again to remove the supernatant. The mature side chains were dried in a vacuum centrifugal concentrator at 30 °C, dissolved in an appropriate volume of DMF, and stored for subsequent use.

## Synthesis of the insulin analogs

The side chains were activated by adding excess HOSU and DCC to the synthesized side chains. The reaction mixture was stirred in DCM as the solvent at room temperature for 1–2 h. After activation, the mixture was filtered through a 0.2 μm organic filter membrane, and the solvent was removed using a vacuum centrifugal concentrator at 30 °C. The residue was suspended in ethyl acetate and filtered again through a 0.2 μm organic filter membrane. The solvent was removed a second time using a vacuum centrifugal concentrator at 30 °C. For deprotection, TFA was added in a volume exceeding 80% of the total mixture, and the reaction was allowed to proceed for 0.5–2 h. Subsequently, isopropyl ether (eight times the volume of the mixture) was added to induce precipitation at -20 °C for 10–30 min. The supernatant was discarded after centrifugation at 8000 rpm for 5 min. The precipitate was washed with additional isopropyl ether, resuspended, centrifuged, and the supernatant was removed. The mature side chains were dried in a vacuum centrifugal concentrator at 30 °C and dissolved in an appropriate volume of DMF for storage.

## In vitro bioactivity assays

CHO-hIR cells were cultured in DMEM complete medium, consisting of fetal bovine serum (50.6 mL), sodium pyruvate (5.6 mL), non-essential amino acid solution (5.6 mL), and methotrexate (MTX) at a concentration of 4 mg/mL (0.56 mL added to 500 mL of DMEM basal medium). The cells were maintained at 37 °C in a 5% $CO_2$ atmosphere until they reached the logarithmic growth phase. Subsequently, the cells were dissociated using

trypsin and seeded into a 96-well cell culture plate at a density of $1.8 \times 10^5$ cells/mL. The plates were incubated at 37 °C with 5% $CO_2$ for 16 to 20 h.

After incubating the cells with compounds at various concentrations (ranging from 100,000 to 0.896 nmol/L) for 30 min at 37 °C, the cells were lysed using cell lysis buffer. The lysate was transferred to a 96-well high-binding plate pre-coated with 6 μg/mL of anti-insulin receptor antibody. The plate was incubated at 37 °C for 3 h and then blocked with 3% BSA for 2 h. After blocking, the wells were washed five times with DELFIA wash solution. A secondary antibody solution (PT66, AD0040, PerkinElmer) at a concentration of 0.3 μg/mL was added and incubated for 1 h, followed by another five washes with DELFIA wash solution. Finally, 200 μL of DELFIA enhancement solution was added to each well and incubated for 2 h.

The 96-well plate was then transferred to a SpectraMax i3x Multi-Mode Microplate Reader (Molecular Devices, USA) for HTRF detection, with excitation and emission wavelengths set at 665 nm and 616 nm, respectively. The acquired data were analyzed using Prism 5 software, plotting the logarithm of compound concentrations on the X-axis and the corresponding fluorescence intensities on the Y-axis. A four-parameter logistic equation was applied for curve fitting, and dose-response curves were generated for both reference and test compounds to calculate their respective $EC_{50}$ values. The relative biological activity of the compounds was assessed by comparing their $EC_{50}$ values to that of icodec.

## In vitro evaluation human serum albumin affinity

The evaluation of HSA affinity was conducted as per the methods described in references[39,40]. HSA was immobilized on NHS-activated Bestarose 4FF beads (Bestchrom). Insulin analogs, prepared at twofold concentrations, were added and incubated with PBS for approximately 1 h at room temperature. The mixture was then centrifuged at 2000 rpm for 5 min, and the supernatant was analyzed using HPLC.

## In vitro pharmacokinetic analysis

The experiments were conducted in compliance with the ethical, moral, and scientific principles set forth in the Helsinki Declaration, China's Good Clinical Practice (GCP) for Drugs, and the Good Clinical Practice guidelines issued by the National Medical Products Administration (NMPA).

The samples were incubated at 37 °C in a temperature-controlled incubator for 0, 1, 4, 24, and 48 h. For the plasma incubation system and sample processing, the final volume of 800 μL consisted of 792 μL of various plasma types and 8 μL of test compounds ($n = 3$). At each time point, 100 μL aliquots were collected, and 200 μL of a reaction termination solution (acetonitrile: methanol = 7:3, v/v) was added to quench the reaction. The samples were vortexed thoroughly and then centrifuged at 12,000 rpm and 4 °C for 10 min. Following centrifugation, 200 μL of the supernatant was collected for LC-MS/MS analysis. LC-MS/MS was utilized to quantify sample concentrations, with the zero-time point serving as the control. The residual percentage of the analyte was calculated based on the peak area, and the resulting data were analyzed.

## In vivo studies

*Animals*

The in vivo experiments were reviewed and approved by the Ethical Committee of Experimental Animals at the Chia Tai Tianqing Pharmaceutical Group. All animal studies adhered to the "Laboratory Animal Management Regulations" of China and the "Guide for the Care and Use of Laboratory Animals" (National Institutes of Health, 2011). Additionally, the experiments were conducted in compliance with the ARRIVE guidelines. Efforts were made to minimize the number of animals used and to reduce their suffering during the experiments. All reagents were of the highest analytical grade or equivalent, and double-distilled water was used exclusively throughout the experimental procedures.

The source of the animals: The study employed SPF-grade ICR mice (male, 6–8 weeks old, 18–20 g) procured from the Qinglongshan Animal Breeding Farm in Jiangning District, Nanjing, China. Additionally, SPF-grade BKS-db/db mice (male, 5–6 weeks old, 30–40 g) were obtained from Jiangsu Jicui Yaokang Biotechnology, China. Beagle dogs (male, 11–13 months old, 10.5 ± 1 kg) were supplied by Jiangsu Laika Biotechnology Co., Ltd., China, and rats (male, 0.17 ± 1 kg) were sourced from Shanghai Bikai Keyi Biotechnology Co., Ltd., China.

Euthanasia method for experimental animals: Animals were euthanized using $CO_2$ asphyxiation. (1) The euthanasia chamber was initially filled with $CO_2$ for 20–30 s, after which the animal was placed inside. (2) $CO_2$ flow was then resumed for 1–5 min until the animal exhibited no movement, cessation of breathing, and dilated pupils. (3) $CO_2$ flow was stopped, and the animal was observed for an additional 2 min to confirm death. (4) Carcasses were placed in opaque plastic bags designated for biohazardous materials, stored at − 20 °C, and subsequently disposed of in compliance with legal regulations for biohazard waste.

## In vivo study in ICR mice

SPF-grade ICR mice (male, 18–20 g) were used in the study. ICR mice were allocated into 10 groups ($n = 4$ per group) based on body weight and baseline blood glucose levels. The groups were designated as follows: Blank control (PBS), Group A (Insulin icodec), Group B (TBE001-A-S008), Group C (TBE001-A-S014), Group D (TBE001-A-S015), Group E (TBE001-A-S033), Group F (TBE001-A-S006), Group G (TBE001-A-S010), Group H (TBE001-A-S029), Group I (TBE001-A-S030), and Group J (TBE001-A-S031). The experimental duration was 72 h. The administration protocol consisted of a single subcutaneous injection of either PBS or insulin analogs at a dose of 1.44 μmol/kg. Blood glucose levels were measured via tail-tip venipuncture at 0, 24, 48, and 72 h post-injection. The glucose-lowering efficacy of the test compounds was evaluated by calculating the area under the curve (AUC0–72 h) for each group. The mice were anesthetized via intraperitoneal injection of 0.25% tribromoethanol at a dose of 125 mg/kg.

### In vivo study in Db/db mice

Db/db mice were allocated into six groups ($n = 4$ per group) based on body weight and blood glucose levels. The groups were designated as follows: Blank control (PBS), Group A (Insulin icodec), Group B (icodec, 3 mg/kg), Group C (icodec, 6 mg/kg), Group D (TBE001-A-S033, 3 mg/kg), and Group E (TBE001-S033, 6 mg/kg). The experiment was conducted over a period of 52 days. Insulin analogs were administered every two days, while the control group received a single subcutaneous injection of PBS. Blood glucose levels were measured every five days, and body weight was recorded weekly. Following the experiment, HbA1c levels and other blood parameters were evaluated. The mice were anesthetized via intraperitoneal injection of 0.25% tribromoethanol at a dose of 125 mg/kg.

### In vivo pharmacokinetic analysis

Beagle dogs were allocated into two groups ($n = 4$ per group) based on body weight. The groups were designated as follows: Group A (Insulin icodec) and Group B (TBE001-A-S033). The experiment duration was 216 h. Whole blood samples (1 mL) were collected from the subcutaneous forelimb vein at predetermined time points post-administration: 0.5, 1, 2, 4, 6, 8, 10, 24, 48, 72, 96, 120, 168, and 216 h. Blood samples were collected in pre-cooled K2 EDTA tubes. A single subcutaneous injection of PBS and insulin analog was administered at a dose of 2 nmol/kg. Plasma was separated by centrifugation at 4,000 rpm and 4 °C for 10 min. The plasma was then transferred to low-adsorption centrifuge tubes and stored at -80 °C until analysis. For analysis, plasma samples were thawed, and 100 µL aliquots were transferred to 1.5 mL low-adsorption centrifuge tubes. Subsequently, 200 µL of internal standard solution was added, and the mixture was vortexed for 3 min. After centrifugation at 12,000 rpm and 4 °C for 10 min, 200 µL of the supernatant was transferred to a 2.2 mL low-adsorption 96-well plate for LC-MS/MS analysis (injection volume: 1 µL). Pharmacokinetic parameters and half-life were calculated using WinNonlin version 8.2 software with a non-compartmental model. The beagles were anesthetized via intravenous injection of propofol at a dose of 5 mg/kg.

SD rats were allocated into two groups ($n = 4$ per group) based on body weight. The groups were designated as follows: Group A (Insulin icodec) and Group B (TBE001-A-S033). The experiment for the rats lasted 96 h. Whole blood samples (1 mL) were collected from the subcutaneous forelimb vein at predetermined time points post-administration: 0.5, 1, 2, 4, 6, 8, 10, 24, 48, 72, and 96 h. Blood samples were collected in pre-cooled K2 EDTA tubes. A single subcutaneous injection of phosphate-buffered saline (PBS) and conjugate was administered at a dose of 2 nmol/kg. Plasma was separated by centrifugation at 4,000 rpm and 4 °C for 10 min. The plasma was then transferred to low-adsorption centrifuge tubes and stored at -80 °C until analysis. For analysis, plasma samples were thawed, and 100 µL aliquots were transferred to 1.5 mL low-adsorption centrifuge tubes. Subsequently, 200 µL of internal standard solution was added, and the mixture was vortexed for 3 min. After centrifugation at 12,000 rpm and 4 °C for 10 min, 200 µL of the supernatant was transferred to a 2.2 mL low-adsorption 96-well plate for LC-MS/MS analysis (injection volume: 1 µL). Pharmacokinetic parameters and half-life were calculated using WinNonlin version 8.2 software with a non-compartmental model. The SD rats were anesthetized via intraperitoneal injection of 0.25% tribromoethanol at a dose of 300 mg/kg.

### Statistical analysis

The data were analyzed using GraphPad Prism version 9.5. Statistical analysis was performed with one-way ANOVA, followed by Dunnett's test for multiple comparisons. The results are expressed as the mean ± standard deviation (SD).

## Data availability

The datasets used and/or analysed during the current study available from the corresponding author on reasonable request.

Received: 19 November 2024; Accepted: 11 March 2025
Published online: 19 March 2025

## References

1. Nishimura, E. et al. Molecular and pharmacological characterization of insulin icodec: A new basal insulin analog designed for once-weekly dosing. *BMJ Open. Diab Res. Care.* **9**(1), e002301. https://doi.org/10.1136/bmjdrc-2021-002301 (2021).
2. Sun, H. et al. IDF diabetes atlas: global, regional and country-level diabetes prevalence estimates for 2021 and projections for 2045. *Diabetes Res. Clin. Pract.* **183**, 109119. https://doi.org/10.1016/j.diabres.2021.109119 (2022).
3. Home, P. D. Plasma insulin profiles after subcutaneous injection: How close can we get to physiology in people with diabetes? *Diabetes Obes. Metab.* **17**(11), 1011–1020. https://doi.org/10.1111/dom.12501 (2015).
4. Karami, H., Shirvani Shiri, M., Rezapour, A., Sarvari Mehrabadi, R. & Afshari, S. The association between diabetic complications and health-related quality of life in patients with type 2 diabetes: A cross-sectional study from Iran. *Qual. Life Res.* **30**(7), 1963–1974. https://doi.org/10.1007/s11136-021-02792-7 (2021).
5. Peyrot, M., Barnett, A. H., Meneghini, L. F. & Schumm-Draeger, P. -M. insulin adherence behaviours and barriers in the multinational global attitudes of patients and physicians in insulin therapy study. *Diabet. Med.* **29** (5), 682–689. https://doi.org/10.1111/j.1464-5491.2012.03605.x (2012).
6. Kjeldsen, T. B. et al. Engineering of orally available, ultralong-acting insulin analogues: discovery of OI338 and OI320. *J. Med. Chem.* **64**(1), 616–628. https://doi.org/10.1021/acs.jmedchem.0c01576 (2021).
7. Kjeldsen, T. B. et al. Molecular engineering of insulin Icodec, the first acylated insulin analog for once-weekly administration in humans. *J. Med. Chem.* **64**(13), 8942–8950. https://doi.org/10.1021/acs.jmedchem.1c00257 (2021).
8. Haraldsson, B., Nyström, J. & Deen, W. M. Properties of the glomerular barrier and mechanisms of proteinuria. *Physiol. Rev.* **88**(2), 451–487. https://doi.org/10.1152/physrev.00055.2006 (2008).
9. Veronese, F. M. & Pasut, G. PEGylation, successful approach to drug delivery. *Drug Discov. Today* **10**(21), 1451–1458. https://doi.org/10.1016/S1359-6446(05)03575-0 (2005).

10. Kurtzhals, P., Østergaard, S., Nishimura, E. & Kjeldsen, T. Derivatization with fatty acids in peptide and protein drug discovery. *Nat. Rev. Drug Discov.* **22**(1), 59–80. https://doi.org/10.1038/s41573-022-00529-w (2023).
11. Ilyushin, D. G. et al. Chemical polysialylation of human recombinant butyrylcholinesterase delivers a long-acting bioscavenger for nerve agents in vivo. *Proc. Natl. Acad. Sci. USA*. **110**(4), 1243–1248. https://doi.org/10.1073/pnas.1211118110 (2013).
12. Scott, L. J. Insulin glargine/lixisenatide: A review in type 2 diabetes. *Drugs* **77**(12), 1353–1362. https://doi.org/10.1007/s40265-017-0783-4 (2017).
13. Vasselli, J. R. et al. Central effects of insulin detemir on feeding, body weight, and metabolism in rats. *Am. J. Physiol.-Endocrinol. Metab.* **313**(5), E613–E621. https://doi.org/10.1152/ajpendo.00111.2016 (2017).
14. Tambascia, M. A. & Eliaschewitz, F. G. Degludec: The new ultra-long insulin analogue. *Diabetol. Metab. Syndr.* **7**(1), 57. https://doi.org/10.1186/s13098-015-0037-0 (2015).
15. Marso, S. P. et al. Efficacy and safety of degludec versus glargine in type 2 diabetes. *N Engl. J. Med.* **377**(8), 723–732. https://doi.org/10.1056/NEJMoa1615692 (2017).
16. Jonassen, I. et al. Design of the novel protraction mechanism of insulin degludec, an ultra-long-acting basal insulin. *Pharm. Res.* **29**(8), 2104–2114. https://doi.org/10.1007/s11095-012-0739-z (2012).
17. Dong, Y. et al. Design of a novel long-acting dual GLP-1/GIP receptor agonist. *Bioorg. Med. Chem.* **100**, 117630. https://doi.org/10.1016/j.bmc.2024.117630 (2024).
18. Lau, J. et al. Discovery of the once-weekly glucagon-like peptide-1 (GLP-1) analogue semaglutide. *J. Med. Chem.* **58**(18), 7370–7380. https://doi.org/10.1021/acs.jmedchem.5b00726 (2015).
19. Sharma, A. K. et al. Insulin analogs: Glimpse on contemporary facts and future prospective. *Life Sci.* **219**, 90–99. https://doi.org/10.1016/j.lfs.2019.01.011 (2019).
20. Philis-Tsimikas, A. An update on the use of insulin detemir, with a focus on type 2 diabetes (drug evaluation update). *Expert Opin. Pharmacother.* **9**(12), 2181–2195. https://doi.org/10.1517/14656566.9.12.2181 (2008).
21. Kalra, S. Insulin degludec: A significant advancement in ultralong-acting basal insulin. *Diabetes Ther.* **4**(2), 167–173. https://doi.org/10.1007/s13300-013-0047-6 (2013).
22. Rosenstock, J. et al. The basis for weekly insulin therapy: Evolving evidence with insulin Icodec and insulin Efsitora Alfa. *Endocr. Rev.* **45**(3), 379–413. https://doi.org/10.1210/endrev/bnad037 (2024).
23. Russell-Jones, D. et al. Once-weekly insulin Icodec versus once-daily insulin degludec as part of a basal-bolus regimen in individuals with type 1 diabetes (ONWARDS 6): A phase 3a, randomised, open-label, treat-to-target trial. *Lancet* **402**(10413), 1636–1647. https://doi.org/10.1016/S0140-6736(23)02179-7 (2023).
24. Hubálek, F. et al. Molecular engineering of safe and efficacious oral basal insulin. *Nat. Commun.* **11**(1), 3746. https://doi.org/10.1038/s41467-020-17487-9 (2020).
25. Hubálek, F. et al. Enhanced disulphide bond stability contributes to the once-weekly profile of insulin Icodec. *Nat. Commun.* **15**(1), 6124. https://doi.org/10.1038/s41467-024-50477-9 (2024).
26. Zaragoza, F. Non-Covalent albumin ligands in FDA-approved therapeutic peptides and proteins: Miniperspective. *J. Med. Chem.* **66**(6), 3656–3663. https://doi.org/10.1021/acs.jmedchem.2c01021 (2023).
27. Østergaard, S. et al. The effect of fatty diacid acylation of human PYY3-36 on Y2 receptor potency and half-life in minipigs. *Sci. Rep.* **11**(1), 21179. https://doi.org/10.1038/s41598-021-00654-3 (2021).
28. Coskun, T. et al. LY3298176, a novel dual GIP and GLP-1 receptor agonist for the treatment of type 2 diabetes mellitus: From discovery to clinical proof of concept. *Mol. Metab.* **18**, 3–14. https://doi.org/10.1016/j.molmet.2018.09.009 (2018).
29. Madsen, K. et al. Structure – Activity and protraction relationship of long-acting glucagon-like peptide-1 derivatives: Importance of fatty acid length, polarity, and bulkiness. *J. Med. Chem.* **50**(24), 6126–6132. https://doi.org/10.1021/jm070861j (2007).
30. Knudsen, L. B. & Lau, J. The discovery and development of liraglutide and semaglutide. *Front. Endocrinol.* **10**, 155. https://doi.org/10.3389/fendo.2019.00155 (2019).
31. Ramírez-Andersen, H. S. et al. Long-acting human growth hormone analogue by noncovalent albumin binding. *Bioconjug. Chem.* **29**(9), 3129–3143. https://doi.org/10.1021/acs.bioconjchem.8b00463 (2018).
32. Van Witteloostuijn, S. B. et al. Neoglycolipids for prolonging the effects of peptides: Self-assembling glucagon-like peptide 1 analogues with albumin binding properties and potent in vivo efficacy. *Mol. Pharm.* **14**(1), 193–205. https://doi.org/10.1021/acs.molpharmaceut.6b00787 (2017).
33. Ward, B. P. et al. Peptide lipidation stabilizes structure to enhance biological function. *Mol. Metab.* **2**(4), 468–479. https://doi.org/10.1016/j.molmet.2013.08.008 (2013).
34. Wu, M. et al. Functionally selective signaling and broad metabolic benefits by novel insulin receptor partial agonists. *Nat. Commun.* **13**(1), 942. https://doi.org/10.1038/s41467-022-28561-9 (2022).
35. Zeng, Z. et al. Di-PEGylated insulin: A long-acting insulin conjugate with superior safety in reducing hypoglycemic events. *Acta Pharm. Sin. B* **14**(6), 2761–2772. https://doi.org/10.1016/j.apsb.2024.02.022 (2024).
36. Moyers, J. S. et al. Preclinical characterization of LY3209590, a novel weekly basal insulin Fc-fusion protein. *J. Pharmacol. Exp. Ther.* **382**(3), 346–355. https://doi.org/10.1124/jpet.122.001105 (2022).
37. Strohl, W. R. Fusion proteins for half-life extension of biologics as a strategy to make biobetters. *BioDrugs* **29**(4), 215–239. https://doi.org/10.1007/s40259-015-0133-6 (2015).
38. Blair, H. A. Insulin Icodec: First approval. *BioDrugs* **38**(5), 717–724. https://doi.org/10.1007/s40259-024-00670-5 (2024).
39. Zhang, J., Dong, Y., Ju, D. & Feng, J. Design, synthesis and biological evaluation of double fatty chain-modified glucagon-like peptide-1 conjugates. *Bioorg. Med. Chem.* **44**, 116291. https://doi.org/10.1016/j.bmc.2021.116291 (2021).
40. Qian, M. et al. Long-acting human Interleukin 2 bioconjugate modified with fatty acids by sortase A. *Bioconjug. Chem.* **32**(3), 615–625. https://doi.org/10.1021/acs.bioconjchem.1c00062 (2021).


## Acknowledgements

We thank the China State Institute of Pharmaceutical Industry (Shanghai, China), Shanghai Duomirui Biotechnology Ltd (Shanghai China), and Nanjing Chia tai Tianqing Pharmaceutical Group Co Ltd (Nanjing, China).

## Author contributions

M.Y.: Conceptualization, Data Curation, Formal Analysis, Investigation, Methodology; C.Z.: Investigation, Software, Visualization, Writing—Original Draft; H.X.: Methodology, Supervision; Y.D.: Supervision, Writing—Review & Editing; H.Z.: Supervision, Writing—Review & Editing; C.X.: Methodology, Supervision; J.F.: Conceptualization, Resources, Supervision, Validation; All authors reviewed the manuscript.

## Declarations

## Competing interests

The authors declare no competing interests.

## Additional information

**Supplementary Information** The online version contains supplementary material available at https://doi.org/10.1038/s41598-025-94014-0.

**Correspondence** and requests for materials should be addressed to J.F.

**Reprints and permissions information** is available at www.nature.com/reprints.

**Publisher's note** Springer Nature remains neutral with regard to jurisdictional claims in published maps and institutional affiliations.